A Letters Journal Exploring the Frontiers of Physics

January 2020

EPL, **129** (2020) 15002
doi: 10.1209/0295-5075/129/15002

www.epljournal.org

Apokamp-type gas discharge phenomenon: Experimental and theoretical backgrounds

Vasily Kozhevnikov[1,2], Andrey Kozyrev[1(a)], Alexander Kokovin[1], Aleksey Sitnikov[1], Eduard Sosnin[1], Victor Panarin[1], Victor Skakun[1] and Victor Tarasenko[1]

[1] *Institute of High Current Electronics - Akademichesky ave. 2/3, 634055 Tomsk, Russia*
[2] *Tomsk State University - Lenina st. 36, 634050 Tomsk, Russia*

received 30 August 2019; accepted in final form 21 January 2020
published online 12 February 2020

PACS 52.30.-q – Plasma dynamics and flow
PACS 52.65.Kj – Magnetohydrodynamic and fluid equation
PACS 52.30.Ex – Two-fluid and multi-fluid plasmas

Abstract – The apokamp discharge is an atmospheric pressure plasma jet generating from the bending point of the discharge channel between high-voltage and floating potential electrodes. The jet propagates perpendicularly to the interelectrode discharge channel for several centimetres without gas convection. Based on the simplified plasma-chemical model of the discharge, a theoretical explanation of the apokamp phenomenon was obtained for the first time. It is shown that the apokamp is a stable plasma quasi-jet formed by the positive streamer mechanism.

Introduction. – In 2016, an uncommon discharge type was first obtained experimentally in the atmospheric pressure air [1]. It was a luminous structure, which is formed near the bending point of the gas discharge channel, almost perpendicular to it. This type of discharge was called "apokamp" (from Greek $\alpha\pi o$, "off", and $\kappa\alpha\mu\pi\nu$, "bend").

Figure 1 shows the experimental setup that had been used in order to obtain an apokamp discharge (a) and a typical photo of the luminous jet (b), (c). As it was shown, to obtain an apokamp it is necessary to ignite a pulse discharge between electrodes 2 and 3, while these conditions have to be satisfied: 1) the applied voltage pulse at needle 2 is of positive polarity; 2) the discharge channel should have a natural or forced bend; 3) the electrode 3 and the discharge channel must be under a potential of several kV w.r.t. the "ground". In fig. 1, these conditions are provided by using a high-voltage generator producing positive polarity pulses with the voltage amplitude of $U_p = 11\,\mathrm{kV}$ at $f = 50\,\mathrm{kHz}$ pulse repetition rate. The natural bending of the discharge channel was obtained by adjusting the angle between electrodes in the range of 120°–140°. As a result, an apokamp 5 in the form of a luminous plasma "jet" is formed near the channel bending point in open atmospheric air. There is a darkened intermediate region between the luminous discharge channel and the beginning of the apokamp jet (fig. 1(c)). This photo was taken with a Canon PowerShot SX 60 HS camera with 1/8″ exposure and ISO 1500 light sensitivity.

To estimate the plasma channel temperature, we introduced various substances into the channel and observed whether they were ignited or melted. In particular, the end of a nichrome wire with a length of 20 mm and a diameter of 0.1 mm was melted (the nichrome melting temperature is 1100–1400 °C). So the lower channel temperature estimate was at least 1000 °C [2].

Apokamp discharges were also experimentally obtained in various gas mixtures other than air (Ar-CO_2, Kr-N_2, Xe-Cl_2, Kr-Cl_2) at pressures below atmospheric [3]. The decrease of the molecular gas admixture deprives jet stability and leads to the transition from jet to volume discharge form. Also the important role of the electronegative gas admixture (mainly oxygen) affecting the formation and the development of apokamp was also noted. In pure gases, especially atomic ones, the apokamp phenomenon was not observed.

At first, we had the assumption that the "apokamp jet" is formed in a pulse-frequency discharge mode, gradually increasing in small steps from pulse to pulse. But high-speed shooting [4] convincingly showed that apokamp in air under normal conditions is an analogue of a positive streamer [5–8]. So a tip of "apokamp jet" propagates into non-ionized gas in a single pulse with characteristic velocities of 100–220 km/s depending on the discharge operating voltage amplitude.

(a) E-mail: kozyrev_andrey_1956@icloud.com

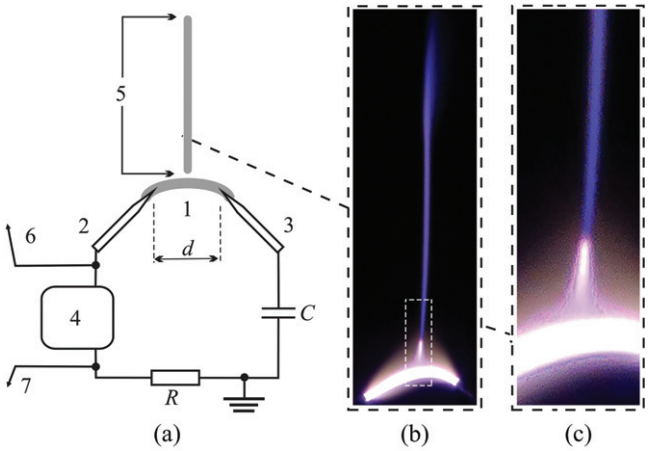

Fig. 1: Experimental setup for the apokamp obtaining under the atmospheric pressure (a), photographic image of the phenomenon (b) and zoomed area between discharge channel and plasma jet (c). 1: discharge gap and plasma channel ($d = 8$ mm); 2, 3: needle electrodes (2 mm diameter and 70 μm tip curvature radius); 4: pulsed voltage source; 5: area of the apokamp formation; 6, 7: terminals for voltage and current measurements, respectively ($C = 3$ pF, $R = 1$ Ohm).

In spite of the wide experimental background we have, the conditions of the apokamp jet initiation remain unclear as well as details of its further development. In particular, so far attempts [9] to simulate the apokamp formation at the theoretical level did not allow to obtain spatio-temporal images of the phenomenon. In this letter, we try to fill up a long-standing lacuna in the theoretical part of this problem, and to perform a deterministic plasma simulation in order to demonstrate the apokamp discharge phenomenon from first principles. Moreover, the purpose of the theoretical study was not the identification of small non-essential details, but the identification of significant processes that ensure the growth of a stable "plasma jet".

Theoretical model. – To understand quantitatively the formation of apokamp starting from the initial stage of the discharge ignition, we have used the "two-moment" non-stationary drift-diffusion macroscopic model [10] implemented in the Plasma module of the COMSOL Multiphysics 5.2a code. The numerical computation routine is based on the finite element method on triangular grid implemented for the macroscopic model equations in log formulation with linear shape functions. The overall number of dimensions of freedom (DOF) does not exceed 2 millions. As a time-dependent solver we used the backward differentiation algorithm (BDF) with variable time step. The relative time-stepping error was equal to 0.0001. We now give a brief overview of the numerical computations.

Since we had very limited computing resources we consider the computational domain to be two-dimensional instead of three-dimensional. It is represented by the rectangular cross-section area 50×70 mm including two parallel blade-shaped electrodes having 0.1 mm curvature radii that are located at an angle of 120 degrees to each other. The interelectrode distance between their tips is equal to 8 mm. The floating potential electrode is modelled as being connected to the ground through the 3 pF capacitance. Another electrode is connected through the $R = 10\,\mathrm{k}\Omega$ ballast load to the high-voltage source producing time-periodic 15 kV amplitude trapezium-shaped pulses of 2.5 μs duration. The electric circuit simulation is consistently implemented by using the SPICE algorithm in COMSOL Multiphysics.

Pure oxygen under the pressure of 1 atm was used as the gas medium in discharge simulations as the most typical representative of pure electronegative molecular gases. The existence of a complete plasma-chemical cross-sections base for oxygen involving a large number of species and reactions [11–13] makes the simulation computationally expensive and not suitable for 2D and 3D models. Different reduction techniques have been proposed by the scientific community to simplify kinetic models of this type. Here we use a minimal set of species and reactions for oxygen including only those enlisted in table 1 from [11–13]. These reactions are necessary to create ion-ion discharge plasma with a small amount of electrons, *i.e.*, typical for electronegative gases.

It is worth commenting specifically on the inclusion in the model of the dissociation reaction of an oxygen molecule (the last reaction in the table). Modeling showed that the absence of this reaction in the plasma model leads to a very high electron temperature and unrealistic rates of impact ionization reaction (the first reaction in the table). Adding a dissociation reaction with a relatively low energy threshold ($\sim$5.6 eV) made the simple model more realistic and ensured a successful modeling of the phenomenon. Here it is essential that this small change is not a very complicated plasma-chemical model, allowing the use of limited computing resources.

Since the apokamp is observed only with a positive polarity of the pulse of the power source, it was necessary to include the mechanism of initiation of secondary free electrons in the gas medium in the model. Photoionization is another important reaction that has to be taken into consideration to simulate plasma jets. We took advantage of the well-known model [9], which allows us to describe the spatial and temporal photoionization of oxygen. In this model the photon-molecule interaction $h\nu + \mathrm{O_2} \rightarrow e + \mathrm{O_2^+}$ is implemented in terms of "differential" representation given as a solution of a Helmholtz set of equations for the photoionization rate reaction. The advantage of photoionization model [14] is its self-sufficiency, and it does not require any expansion of our plasma-chemical scheme.

Gas discharge channel simulation. – In this paper, the simulation of the apokamp initiation phenomenon is carried out for a single pulse from the voltage source, since the experiment indicates that apokamps are a sequence of

Table 1: Reactions included in the model. For electron reactions T_e is the electron temperature in eV.

Reaction	Rate reaction (T_e in eV)	Ref.
$e + O_2 \rightarrow 2e + O_2^+$	$2.3 \cdot 10^{-9} T_e \exp(-12.3/T_e)$ [cm^3/s]	[11]
$e + 2O_2 \rightarrow O_2 + O_2^-$	$2 \cdot 10^{-29}(0.03/T_e)$ [cm^6/s]	[11,12]
$O_2^+ + O_2^- + O_2 \rightarrow 3O_2$	$2 \cdot 10^{-25}$ [cm^6/s]	[11,12]
$e + O_2 \rightarrow e + 2O$	$4.2 \cdot 10^{-9} \exp(-5.6/T_e)$ [cm^3/s]	[13]

fast moving "plasma bullets", *i.e.*, positive streamers moving in a pre-prepared plasma environment [4]. Namely, during the first 100–200 voltage pulses, which follow at ∼25–50 kHz repetition frequency, a spark ignition occurs between the electrodes multiple times, accompanied by the heating of near-electrode space to temperatures above 1100–1300 °C, the appearance of surrounding luminous halo and bending of the main discharge channel without an apokamp growth.

To simulate starting conditions for the initial preionization and after fixing the neutral gas pre-heating, the symmetric temperature and the number density of the quasi-neutral ion-ion plasma in the form of "Gaussian spots" have been set. The background temperature is equal to $T_0 = 300$ K and the background plasma number density is $n_0 \sim 10^3$ cm^{-3}, the maximal temperature of the main discharge channel $T_{\max} = 1100$–1300 °C is obtained from experimental data, while the maximal number density $n_{\max} \sim 10^{12}$ cm^{-3} corresponds to typical plasma density values for self-sustained atmospheric discharge. Note that the proposed model does not consider explicitly the gas heating process just using a constant pre-defined temperature field instead. The position for the plasma initial "spot" is chosen straight in the middle of the interelectrode gap. The initial plasma distribution is an elliptical spot stretched horizontally taken as the closest shape to the real plasma channel generated by a large number of voltage pulses repetitions. The same has been done for the heating profile *i.e.*, located slightly above the distance between the electrodes tips.

Setting a preliminary temperature profile distribution in our simulations, as well as the initial plasma distribution, is only intended to observe the intial formation and growth of the apokamp channel during one single voltage pulse. A more accurate and complicated simulation combining the discharge plasma modelling with a simulation of the temperature field change was also carried out. Naturally, it requires more computational resources along with setting greater simulation end time. But it leads to a similar temperature distribution as specified above using the simple Gaussian profile. The model temperature distribution is consistent with the experimental measurements in the main discharge channel [4]. The additional temperature definition in the region of possible apokamp plasma jet growth is redundant, since as it is known from

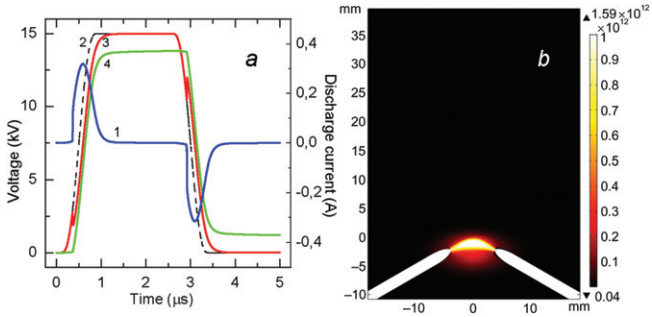

Fig. 2: Pulse-periodic gas discharge: (a) current/voltage time-profiles (1: discharge current, 2: source voltage, 3: potential electrode voltage, 4: floating electrode voltage); (b) image of the quasi-stationary plasma distribution.

experiments the apokamp channel is almost not heated in comparison with other discharge regions.

Figure 2 shows the simulation results in the framework of the theoretical model proposed above. The discharge time profiles (fig. 2(a)) are distinctive for the current flow in a two-electrode system with a floating potential electrode. When voltage is applied to the high-voltage electrode discharge ignition occurs along with simultaneous charging of capacitance connected to the second electrode. After the capacitance is charged to the potential value of the first electrode, the discharge quenches. It ignites again only after the significant decrease of the source voltage so the gap voltage drop reaches the breakdown value. As can be seen from curves 3 and 4, the voltage drop on the quasi-stationary discharge channel is maintained at ∼1 kV.

In fig. 2(b), the discharge channel has a typical bend and a plasma halo is surrounding the near-electrode space according to the experimental pictures (fig. 1(c)). But there is no formation of a plasma jet from the bending area of the discharge channel. This distribution of the plasma (in the channel form without apokamp) remains unchanged during the simulation process, even if we continue to apply pulsed repetition voltage up to tens and hundreds of short pulses.

Apokamp jet simulation. – Since the experiments clearly show that the nature of the phenomenon is not connected to gas convection, it becomes obvious that apokamp formation requires an external electric field directed perpendicular to the main discharge channel.

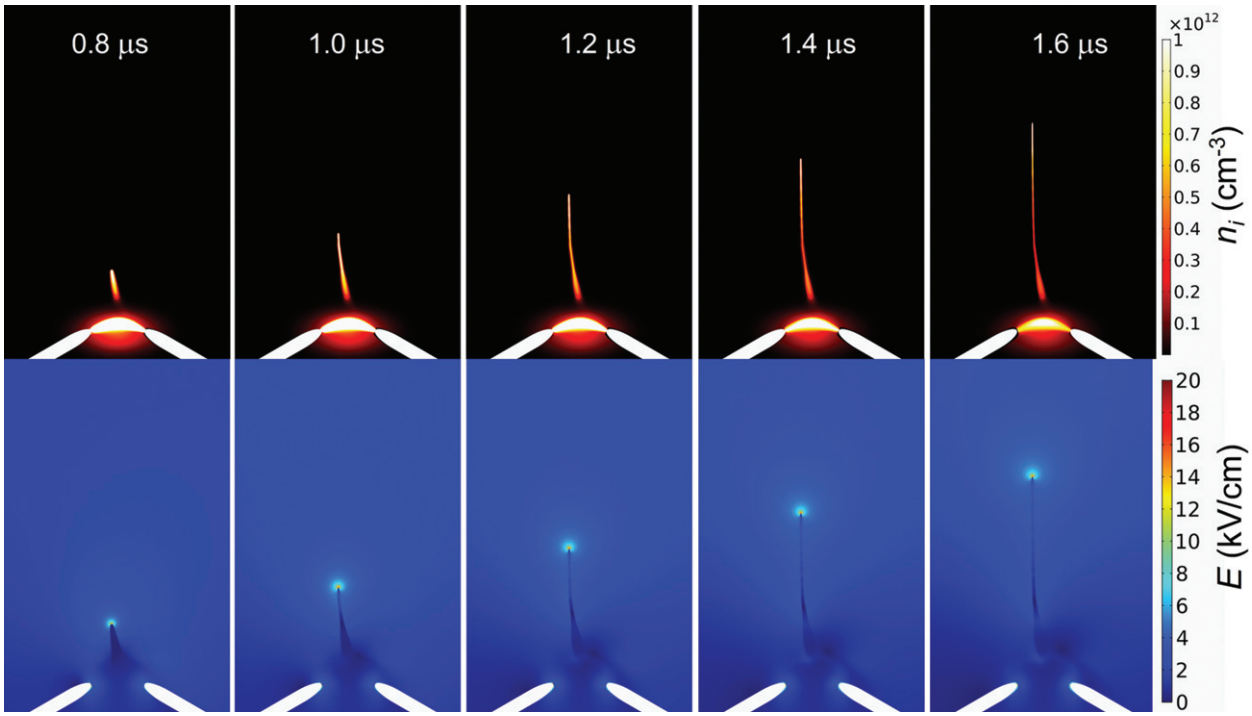

Fig. 3: The sequences of frames illustrating the phenomenon of apokamp growth during a single voltage pulse: distribution of ion-ion plasma (top row) and the absolute value of electric field strenght (lower row). The distance between the tips of the electrodes is 8 mm. Time is counted from the moment the voltage pulse is applied as in fig. 2.

To determine the role of a weak external transverse electric field the electric potential of the upper boundary of the computational domain was set to zero (became grounded). As the discharge channel between metal electrodes was located at a distance of about 60 mm from the upper boundary of the computational domain, so the difference in electric potentials was approximately ten times less than the breakdown voltage for this gap. Nevertheless, the presence of a third electrode, placed far from the discharge, led to the appearance of a weak transverse electric field and the apokamp growth development. An estimate of our average electric field strength at the level of 15 kV/6 cm = 2.5 kV/cm just corresponds to the known level of minimum fields for the development of a positive streamer [5]. Below, for the first time, theoretically calculated images of a positive streamer starting not from the electrode, but from the place of bending of the plasma channel are shown.

Figure 3 shows the time dynamics of the main discharge ignition followed by the plasma halo formation and growth of the apokamp jet towards the far (upper) electrode. For a more detailed description of this phenomenon, both the distribution of plasma components and the absolute value of an electric field are given in fig. 3. To better demonstrate the spatially inhomogeneous structure of the apokamp jet, the number density scale was selected in a reduced range, therefore, the main discharge channel in the frames (upper row of fig. 3) looks overexposed.

The growth of the apokamp jet (fig. 3) occurs during a period of time less than one voltage pulse duration. The "appendix", *i.e.*, base of apokamp, starts at the 500 ns time point after the main discharge ignition. There is a less dense ($\sim 5 \cdot 10^{11}\,\mathrm{cm}^{-3}$) region between the dense plasma of the main discharge channel and the nascent apokamp appendix. The appendix appears in the region where the electric field reaches its relative maximum value between the conditional boundary of plasma halo and the surrounding non-ionized gas. Further apokamp development occurs due to the intensive oxygen photoionization typical of the dynamics of a positive streamer [5,6]. Both the appendix and the whole apokamp jet are made of dense oxygen plasma ($\sim 10^{13}\,\mathrm{cm}^{-3}$), mainly constituted by positive and negative ions.

In the bottom row of fig. 3 the distribution of the electric field (absolute value) is depicted. Due to the sufficient number density of ion-ion plasma inside the body of the growing jet, the high potential of the discharge channel is carried to the tip of the jet. In fig. 3 (bottom row) it is clearly seen that the field strength inside the apokamp body is close to zero. In the same time the tip of the apokamp jet is having the high value of the electric field of ~20 kV/cm. This field is sufficient for intense impact ionization to ensure the apokamp tip propagates into a non-ionized gas medium.

In order to vividly demonstrate the complex spatial structure of the apokamp jet, fig. 4 shows (in an enlarged scale) the instantaneous distributions of the number density of free electrons, negative ions (here, it is only O_2^-), and field strength at a time point of 1 μs. It can be seen that the electron number density reaches its maximum

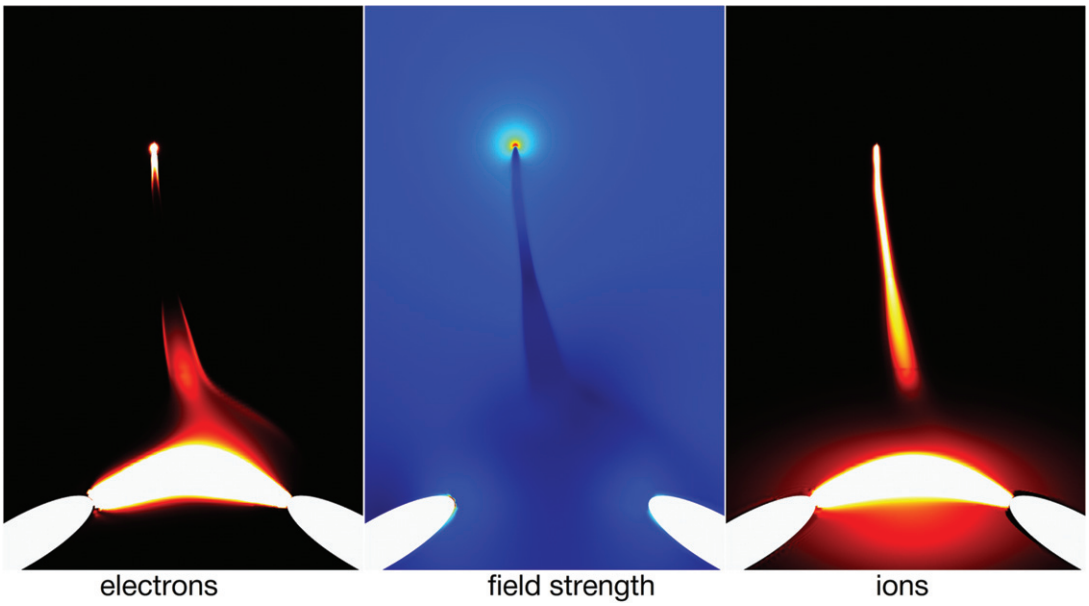

Fig. 4: Detailed spatial distribution of free electrons, electric field strenght and ion-ion plasma at 1.0 μs time point.

only at the tip of the growing apokamp channel. The rapid electron attachment leaves ion-ion ($O_2^+ + O_2^-$) plasma inside the growing streamer channel.

It is known that the local amplification coefficient, K, of the electric field at the top of a long conductive rod strongly depends on the ratio of the length of the rod, l, to the radius of its cross section, $r \ll l$, namely, $K \sim l/r$ [15]. Just the small transverse size of the channel, r, provides a sufficient level of the weak external field amplification to the breakdown field value at the top of the growing apokamp channel.

Because of its relatively low mobility, ion-ion plasma is capable of providing a sufficiently small transverse jet size, r, which determines a high field gain, K. Quite likely, in non-attaching gases, the apokamp is either not observed at all, or is not so clearly marked due to the rapid expansion of electron-ion plasma in the transverse direction.

In our model, we did not calculate the excitation of atoms and molecules, as well as any irradiative characteristics of the plasma. But we are sure that increased electron number density at the tip facilitates the excitation of atomic levels leading to the short-term localized luminescence of the corresponding region. Visually, on high-speed photography such regions look like plasma clots or plasma "bullets" that are experimentally observed in this phenomenon at atmospheric pressure [4]. In our example, the tip of jet propagates at a speed of 35 km/s. It is in a good agreement with experimental data, especially taking into account the highly simplified plasma model.

Conclusions. – We have presented a first-of-a-kind simulation of the apokamp discharge phenomenon that was discovered previously in experiments. As a theoretical model of the gaseous medium, a simplified plasma-chemical scheme was taken, and the quantitative cross-sections correspond to elementary processes in oxygen. The simulation has demonstrated that apokamp is a phenomenon arising in a weak external electric field and originating from the main channel of the gas discharge with a floating potential electrode. If these conditions are met, the resulting apokamp jet has a stable electro-negative plasma structure and propagates into the non-ionized regions with high speeds, creating significant electric fields on the tip. The simulation convincingly explains the details of the apokamp jet formation shown in experiments, such as the "plasma bullets" propagation in the apokamp channel, recorded by high-speed imaging. Also, the simulation revealed a nontrivial spatial structure of the apokamp jet, which is established at earlier stages of jet formation.

Based on the electrical and optical measurements of the apokamp discharge parameters, as well as from the theoretical simulation results, we can draw the following brief conclusions.

1) The apokamp is a narrow streamer channel growing at characteristic velocities from 20 up to 200 km/s (depending on the applied voltage, pressure and neutral gas type) from the bending point of a discharge in a pulse-repetition mode. The bending region provides a local electric field enhancement setting the initial anisotropy of the starting streamer.

2) The necessary conditions for an extended streamer channel growing are created by a relatively weak (~2 kV/cm, an order lower than static breakdown value) macroscopic electric field maintained between the high-voltage discharge channel and the far zero-potential surrounding space. This low average field enhances at the growing streamer head to the

near-breakdown values (∼20 kV/cm, which is about 70% of the static breakdown threshold according to the Paschen curve), ensuring its rapid growth due to local gas ionization.

3) Although we cannot yet simulate a long pulse-periodic regime of the apokamp phenomenon, we can assume the preceding ion-ion plasma core provides a reproduction of the channel shape and direction from pulse to pulse. Therefore, the pulse-periodic mode discharge looks like a continuous plasma jet with a characteristic shape tied to the bend of the main discharge channel.

* * *

This work was supported by the Russian Foundation for Basic Research (RFBR) grant No. 19-08-00286.

REFERENCES

[1] Sosnin E. A., Skakun V. S., Panarin V. A., Pechenitsin D. S., Tarasenko V. F. and Baksht E. K., *JETP Lett.*, **103** (2016) 761.
[2] Sosnin E. A., Andreev M. V., Didenko M. V., Panarin V. A., Skakun V. S. and Tarasenko V. F., *High Temp.*, **56** (2018) 837.
[3] Kuznetsov V. S., Sosnin E. A., Panarin V. A. Skakun V. S. and Tarasenko V. F., *Opt. Spectrosc.*, **125** (2018) 324.
[4] Sosnin E. A., Panarin V. A., Skakun V. S., Baksht E. K. and Tarasenko V. F., *Eur. Phys. J. D*, **71** (2017) 25.
[5] Allen N. L. and Mikropoulos P. N., *J. Phys. D: Appl. Phys.*, **32** (1999) 913.
[6] Qin J. and Pasko V. P., *J. Phys. D: Appl. Phys.*, **47** (2014) 435202.
[7] Naidis G. V., *JETP*, **82** (1996) 694.
[8] Heijmans L. C. J., Nijdam S., van Veldhuizen E. V. and Ebert U., *EPL*, **103** (2013) 25002.
[9] Babaeva N. Yu. and Naidis G. V., *Phys. Plasmas*, **23** (2016) 083527.
[10] Gogolides E. and Sawin H. H., *J. Appl. Phys.*, **72** (1992) 3988.
[11] Lieberman M. A. and Lichtenberg A. J., *Principle of Plasma Discharges and Materials Processing* (Wiley, New York) 2005.
[12] Kossyi I. A., Kostinsky A. Yu., Matveyev A. A. and Silakov V. P., *Plasma Sources Sci. Technol.*, **1** (1992) 207.
[13] He J. and Zhang Y. T., *Plasma Process. Polym.*, **9** (2012) 9.
[14] Bourdon A., Pasko V. P., Liu N. Y., Célestin S., Ségur P. and Marode E., *Plasma Sources Sci. Technol.*, **16** (2007) 656.
[15] Chatterton P. A., *Proc. R. Soc.*, **88** (1966) 231.